Characterization of Soil Particle Size Distribution with a Fractal Model in the Desertified Regions of Northern China

Guang-Lei GAO[1,2], Guo-Dong DING[1,2], Yuan-Yuan ZHAO[1,2], Bin WU[1,2], Yu-Qing ZHANG[1,2], Jian-Bin GUO[1,2], Shu-Gao QIN[1,2], Yan-Feng BAO[1], Ming-Han YU[1], and Yun-Dong LIU[1]

[1]Yanchi Research Station, School of Soil and Water Conservation, Beijing Forestry University, Beijing, P.R. China

[2]Key Laboratory of Soil and Water Conservation and Desertification Combating, Ministry of Education, Beijing Forestry University, Beijing, P.R. China; e-mail: dingguodong@bjfu.edu.cn

A b s t r a c t

We constructed an aeolian soil database across arid, semi-arid, and dry sub-humid regions, China. Soil particle size distribution was measured with a laser diffraction technique, and fractal dimensions were calculated. The results showed that: (i) the predominant soil particle size distributed in fine and medium sand classifications, and fractal dimensions covered a wide range from 2.0810 to 2.6351; (ii) through logarithmic transformations, fractal dimensions were significantly positive correlated with clay and silt contents ($R^2 = 0.81$ and 0.59, $P < 0.01$), and significantly negative correlated with sand content ($R^2 = 0.50$, $P < 0.01$); (3) hierarchical cluster analysis divided the plots into three types which were similar to sand dune types indicating desertification degree. In a large spatial scale, fractal dimensions are still sensitive to wind-induced desertification. Therefore, we highly recommend that fractal dimension be used as a reliable and quantitative parameter to monitor soil environment changes in desertified regions. This improved information provides a firm basis for better understanding of desertification processes.

Key words: desertification, aeolian soil, particle size distribution, fractal dimension.

1. INTRODUCTION

Desertification means land degradation in arid, semi-arid, and dry sub-humid areas resulting from various factors including climatic variations and human activities (UNEP 1994). In China, desertified lands usually lie in the regions above 35° N with an annual precipitation < 450 mm (Wang *et al.* 2008). The latest *Bulletin by the State Forestry Administration*, P.R. China, has declared that desertification regions in China cover 2.62 million km^2, accounting for more than 27% of the total landmass (SFA 2011). Desert expansions and remediation strategies have already been studied in China (Chen and Tang 2005, Wang *et al.* 2008). However, land desertification does not only cause expansions of desert landscape, but also soil structure damage and functional losses on a smaller scale (Zha and Gao 1997). Therefore, the recovery of soil structures and functions to sustain plant and animal life and desert ecosystem development has drawn increasing attention recently (Duan *et al.* 2004, Li *et al.* 2007, Chen and Duan 2009, Jiao *et al.* 2011).

Soil particle size distribution (PSD) is one of the fundamental attributes of soil systems (Hillel 1980). Soil PSD affects the movement and retention of water, solutes, heat, and air (Su *et al.* 2004), and is widely used as a basis for estimating soil texture, organic carbon, nutrients, and hydraulic properties (Tyler and Wheatcraft 1990, Skaggs *et al.* 2001 Arrouays *et al.* 2006, Reynolds *et al.* 2006). Therefore, characterizing soil PSD with a single index that retains more information, as well as changes that occur due to desertification, is an approach of great interest when dealing with soil data (Su *et al.* 2004).

Numerous studies have developed mathematical models for estimating soil PSD (Buchan 1989, Nemes *et al.* 1999, Skaggs *et al.* 2001, Hwang *et al.* 2002). However, in these studies, the irregular and nonlinear structures of soil systems have been simply ignored as indescribable, although they could provide a much better representation of many natural phenomena (Mandelbrot 1983). In the 1960s, Mandelbrot (1967) created fractal geometry to describe the complex natural world, characterized by irregularity, self-similarity, and nonlinearity, and firstly provided a fractal model to describe soil PSD and its variations (Mandelbrot 1983). Following this, fractal arithmetic was more and more often applied to identify soil PSD and additional environmental changes (Turcotte 1986, Tyler and Wheatcraft 1992, Crawford *et al.* 1993, Wang *et al.* 2005, Gao *et al.* 2014a). Among these studies, the common feature of fractal measurements is the use of fractal dimensions to characterize soil PSD (Gui *et al.* 2010). The latest studies of soil systems on the fractal dimensions of PSD have demonstrated that fractal dimensions significantly correlate with the various soil particles contents, and imply the variations in soil porosity, organic matter, and nutrient content following a

linear trend (Su *et al.* 2004, Liu *et al.* 2009, Gui *et al.* 2010, Jin *et al.* 2013, Gao *et al.* 2014b). Fractal dimensions are considered to be more sensitive than soil texture, organic matter, as well as fertility in reflecting the variations in soil systems (Su *et al.* 2004, Fu *et al.* 2009), and become important in understanding and quantifying soil degradation and dynamics on different spatial scales (Jin *et al.* 2013). However, former studies have always focused on the variations in fractal dimensions on a smaller spatial scale; the uncertainty of variation on a larger spatial scale creates space for further developments of the use of fractal dimensions.

In desertification regions, wind-induced changes in soil PSD are drastic. Frequent and intense wind erosion sorts soil fractions, removing fine particles and leaving coarse-textured soil behind (Lobe *et al.* 2001). In this paper, we analyzed soil PSD and the fractal dimensions of topsoil from the desertified regions of northern China. The objectives of this study were: (i) to characterize soil PSD using fractal dimensions, (ii) to examine if fractal dimensions of soil PSD can represent the variations in soil systems over a large spatial scale, and (iii) additionally to assess desertification trends and the efforts of anti-desertification solutions in desertified regions of northern China.

2. MATERIAL AND METHODS

2.1 Soil information

A soil database was established from the field-based investigation of aeolian topsoil. It included 39 sampling plots from 7 field stations covering Horqin Sandland, Mu Us Sandland, Kubuqi Desert, Tengger Desert, Hexi Desert, and Gurbantunggut Desert across arid, semi-arid, and dry sub-humid regions of northern China (Table 1). In each sampling field, 3 sub-plots were selected for topsoil sample collection; in each sub-plot, 5 topsoil samples were randomly collected at a depth of 0-5 cm. Additionally, the sampling positions were all on the flat tops of sand dunes to eliminate the effects of microphysiognomy. In total, 585 topsoil samples qualified.

2.2 Soil analysis

All soil samples were air-dried and passed through a 2 mm sieve prior to laboratory analysis. To indentify soil PSD information, the topsoil samples were pretreated in an H_2O_2 solution (30%, w/w) to destroy organic matter. Then, soil aggregates were dispersed by adding sodium hexametaphosphate (NaHMP) and sonicatied for 30 s (Wang *et al.* 2006, Gui *et al.* 2010). Finally, soil PSD data was obtained with a laser diffraction technique using a Malvern Instrument MS 2000 (Malvern, England) with a measurement range and error of 0.02-2000 μm and < 2%, respectively. Each sample was meas-

General information of the selected plots
in arid and semi-arid regions of northern China

Plot	Land use	Sand dune	Vegetation type	Planta-tion duration [years]	Soil type	Altitude [m]	Location	Region
1	Woodland	Fixed	*Pinus sylvestnis*	35	Aeolian soil	207	N42°41.15′, E122°33.1′	Horqin Sandland
2	Woodland	Fixed	*Pinus densiflora*	35	Aeolian soil	209	N42°41.03′, E122°33.3′	Horqin Sandland
3	Woodland	Fixed	*Pinus densiflora var zhanguensis*	22	Aeolian soil	203	N42°41.22′, E122°33.87′	Horqin Sandland
4	Grassland	Semi-mobile	*Caragana microphylla*	–	Aeolian soil	244	N42°48.10, E122°33.10′	Horqin Sandland
5	Farmland	–	*Zea mays*	25	Aeolian soil	240	N42°48.07′, E122°33.17′	Horqin Sandland
6	Grassland	Semi-mobile	*Artemisia halodendron*	–	Aeolian soil	358	N42°56.40′, E120°42.97′	Horqin Sandland
7	Woodland	Semi-mobile	*Populus simonii*	14	Aeolian soil	435	N42°33.18′, E120°27.23′	Horqin Sandland
8	Woodland	Semi-mobile	*P. simonii, Hedysarum fruticosum*	7	Aeolian soil	625	N42°23.83′, E119°47.30′	Horqin Sandland
9	Shrubland	Fixed	*H. fruticosum*	11	Aeolian soil	611	N42°23.89′, E119°47.64′	Horqin Sandland
10	Shrubland	Semi-mobile	*C. microphylla*	11	Aeolian soil	610	N42°23.89′, E119°47.64′	Horqin Sandland
11	Shrubland	Semi-mobile	*C. microphylla*	29	Aeolian soil	491	N42°59.94′, E119°39.75′	Horqin Sandland
12	–	Mobile	*Salix gordejevii, H. fruticosum*	16	Aeolian soil	581	N43°04.27′, E119°16.81′	Horqin Sandland
13	Woodland	Fixed	*Pinus tabuliformis*	25	Aeolian soil	1396	N39°18.64′, E109°49.22′	Mu Us Sandland
14	Shrubland	Semi-mobile	*Salix psammophila*	39	Aeolian soil	1340	N39°11.13′, E109°46.97′	Mu Us Sandland
15	Shrubland	Semi-mobile	*H. fruticosum*	27	Aeolian soil	1323	N39°08.17′, E109°44.02′	Mu Us Sandland
16	Shrubland	Semi-mobile	*Artemisia sieversiana, H. fruticosum*	34	Aeolian soil	1336	N39°08.09′, E109°32.04′	Mu Us Sandland
17	Shrubland	Fixed	*Sabina vulgaris*	—	Aeolian soil	1304	N38°58.86′, E109°18.16′	Mu Us Sandland
18	Shrubland	Semi-mobile	*H. fruticosum*	10	Aeolian soil	1386	N38°54.86′, E108°23.71′	Mu Us Sandland

Table 1 (continuation)

Plot	Land use	Sand dune	Vegetation type	Planta-tion duration [years]	Soil type	Altitude [m]	Location	Region
19	Shrubland	Semi-mobile	*Salix cheilophila*	–	Aeolian soil	1419	N38°56.67′, E108°08.75′	Mu Us Sandland
20	Shrubland	Fixed	*Caragana korshinskii*	12	Aeolian soil	1476	N39°33.79′, E108°40.44′	Mu Us Sandland
21	Grassland	Fixed	*Phragmites communis*	–	Aeolian soil	1522	N37°42.40′, E107°14.18′	Mu Us Sandland
22	–	Mobile	*Agriophyllum squarrosum*	–	Aeolian soil	1545	N37°42.00′, E107°13.19′	Mu Us Sandland
23	Woodland	Semi-mobile	*P. sylvestnis*	12	Aeolian soil	1520	N37°42.49′, E107°13.85′	Mu Us Sandland
24	Shrubland	Semi-mobile	*Salix mongolica*	12	Aeolian soil	1519	N37°42.48′, E107°13.68′	Mu Us Sandland
25	Shrubland	Semi-mobile	*Hedysarum mongolicum*	–	Aeolian soil	1501	N37°42.88′, E107°14.10′	Mu Us Sandland
26	Shrubland	Fixed	*C. korshinskii*	27	Aeolian soil	1478	N37°43.87′, E107°13.12′	Mu Us Sandland
27	Shrubland	Fixed	*C. korshinskii*	11	Aeolian soil	1463	N37°43.65′, E107°14.17′	Mu Us Sandland
28	Shrubland	Fixed	*C. korshinskii*	7	Aeolian soil	1487	N37°43.23′, E107°13.89′	Mu Us Sandland
29	Shrubland	Semi-mobile	*H. fruticosum, A. sieversiana*	14	Aeolian soil	1213	N40°16.37′, E108°30.64′	Kubuqi Desert
30	–	Mobile	–	–	Aeolian soil	1075	N40°39.07′, E108°25.30′	Kubuqi Desert
31	Shrubland	Semi-mobile	*Artemisia ordosica*	12	Aeolian soil	1349	N37°28.28′, E105°00.15′	Tengger Desert
32	Shrubland	Semi-mobile	*Hedysarum scoparium*	12	Aeolian soil	1337	N37°28.11′, E104°59.65′	Tengger Desert
33	Shrubland	Semi-mobile	*Haloxylon ammodendron*	24	Aeolian soil	1337	N39°21.09′, E100°07.90′	Hexi Desert
34	Shrubland	Semi-mobile	*Calligonum mongolicunl*	22	Aeolian soil	1356	N39°21.13′, E100°08.17′	Hexi Desert
35	–	Mobile	–	–	Aeolian soil	1384	N39°21.24′, E100°07.80′	Hexi Desert
36	Shrubland	Semi-mobile	*Calligonum mongolicunl*	9	Aeolian soil	514	N44°36.31′, E088°07.77′	Gurbantunggut Ds.
37	Shrubland	Semi-mobile	*H. ammodendron*	30	Aeolian soil	475	N44°22.48′, E087°55.39′	Gurbantunggut Ds.
38	Shrubland	Semi-mobile	*H. ammodendron*	18	Aeolian soil	653	N44°11.73′, E089°32.75′	Gurbantunggut Ds.
39	Shrubland	Semi-mobile	*H. ammodendron*	13	Aeolian soil	678	N44°56.90′, E088°32.63′	Gurbantunggut Ds.

ured 5 times and the arithmetic mean value was calculated and recorded. The analysis results of soil PSD were output with regards to the U.S. Soil Taxonomy of soil particle classification: 0-2, 2-50, 50-100, 100-250, 250-500, 500-1000, and 1000-2000 μm. Further, clay, silt, and sand fractions were defined as 0-2, 2-50, and 50-2000 μm, respectively. Additionally, in this study, soil PSD refers to volume-base data.

2.3 Data processing

Based on the soil PSD data, volume-based fractal dimensions of soil PSD were subsequently calculated according to the fractal model of Wang *et al.* (2005) and Gui *et al.* (2010). The equation is expressed as:

$$\frac{V(r < R_i)}{V_T} = \left(\frac{R_i}{R_{\max}}\right)^{3-D} , \tag{1}$$

where r is the soil particle size, R_i is the soil particle size of grade i, $R_{\max}$ is the maximum value of soil particle size, $V(r < R_i)$ is the volume of soil particle size less than R_i, V_T is the total volume of soil particles, D is the volume-based fractal dimension.

In this study, the field plot and sub-plot were used as the basic study unit. The mean values of soil PSD data and fractal dimensions were identified for statistical analysis. Linear regression, hierarchical cluster and correlation analysis were performed to identify the relationships between D and soil particle fractions. Correlation analysis passed a 2-tailed test to distinguish the significant difference when evaluated at the level of $P < 0.01$. All statistical analyses were conducted using the SPSS software (Version 17.0).

3. RESULTS AND DISCUSSIONS

3.1 Soil PSD and fractal dimension of soil PSD

Based on the data measured by the Malvern Laser Diffraction Instrument, 39 groups of soil PSD were classified (Table 2). There were considerable differences in soil PSD among the 39 field plots. Furthermore, although there was large variability due to the differences in climate, desertification degree, as well as vegetation restoration solutions, the dominant soil particle classification was the size of sand particles. Among them, fine sand and medium sand dominate sand particles, accounting for 39.59 and 22.02% of total fractions, respectively. Accordingly, the content of clay fractions was much lower, ranging from 0.00 to 8.18% (mean value of 1.63%). Soils of this nature are classified as aeolian soil, which is commonly found in arid, semi-arid, and dry sub-humid regions of northern China. This finding resulted from long term wind-induced soil erosion and was consistent with the earlier

Table 2

Soil PSD and fractal dimensions of soil PSD of different field station

Plot	Clay [%]	Silt [%]	Sand [%]	D
1	2.86±0.25	33.91±7.99	59.88±8.24	2.4182±0.0701
2	3.33±0.36	38.45±0.84	58.22±0.71	2.3606±0.0314
3	3.11±0.54	37.83±5.10	59.05±5.33	2.3880±0.1572
4	1.34±0.11	15.49±2.45	83.16±2.40	2.3376±0.0057
5	1.86±0.62	14.65±6.62	83.49±7.19	2.4007±0.0794
6	1.51±0.57	15.55±5.86	82.95±6.36	2.3658±0.0105
7	1.13±0.19	10.66±1.50	88.21±1.69	2.3968±0.0252
8	1.50±0.50	15.67±5.23	82.84±5.73	2.4414±0.0464
9	2.90±1.25	24.96±8.95	72.14±10.21	2.5153±0.0468
10	0.79±0.15	11.32±1.47	87.89±1.57	2.3695±0.0214
11	0.75±0.16	7.76±0.86	91.48±1.01	2.2655±0.0298
12	0.08±0.14	0.67±1.15	99.25±1.29	2.1685±0.0855
13	3.17±0.12	27.65±2.31	69.18±2.23	2.5123±0.0025
14	1.61±0.23	16.24±2.22	82.15±2.40	2.4062±0.0190
15	1.06±0.27	9.50±1.51	89.44±1.74	2.3365±0.0386
16	1.54±0.27	16.43±2.57	82.02±2.81	2.3991±0.0281
17	3.15±0.41	38.67±4.31	58.18±4.29	2.5253±0.0172
18	0.71±0.09	6.09±0.66	93.20±0.73	2.2580±0.0182
19	2.24±0.40	18.97±2.21	78.90±2.51	2.4717±0.0128
20	2.12±0.40	18.97±2.21	78.90±2.51	2.4480±0.0274
21	0.77±0.35	6.48±0.10	92.75±0.26	2.2514±0.0745
22	0.09±0.16	1.46±2.48	98.44±2.64	2.0810±0.0421
23	0.32±0.37	4.54±4.34	95.14±4.70	2.1742±0.0848
24	0.24±0.04	5.92±0.05	93.84±0.09	2.1901±0.0684
25	0.49±0.35	5.76±0.65	93.76±0.92	2.2641±0.0283
26	6.58±1.49	62.41±10.87	31.01±12.35	2.6351±0.0363
27	4.08±0.03	30.94±2.92	64.99±2.89	2.5484±0.0027
28	3.34±0.19	50.06±4.17	46.60±4.36	2.5408±0.0109
29	2.68±0.06	9.81±0.70	87.51±0.75	2.4503±0.0010
30	0.00±0.00	0.00±0.00	100.00±0.00	2.1766±0.0217
31	0.17±0.30	4.21±3.74	95.62±3.95	2.2407±0.0402
32	0.82±0.12	5.48±0.71	93.70±0.76	2.2672±0.0221
33	2.81±0.55	10.37±0.94	86.82±1.49	2.4535±0.0297
34	1.83±0.09	5.96±0.49	92.21±0.57	2.3801±0.0090
35	0.11±0.18	0.22±0.38	99.67±0.57	2.1678±0.0804
36	0.61±0.55	3.99±2.87	95.39±3.42	2.2558±0.0551
37	1.56±0.04	10.84±2.54	87.61±2.54	2.3790±0.0087
38	0.30±0.41	2.99±2.63	96.72±2.95	2.1525±0.1334
39	0.00±0.00	0.18±0.26	99.82±0.26	2.2059±0.0607

studies on the basic mechanical composition of aeolian soil in China (Su *et al.* 2004, Ding 2010).

Table 2 shows the calculated *D* values when Eq. 1 was applied to each soil data set. The *D* values covered a wide range from 2.0810 to 2.6351. Although changes in *D* values varied significantly, there was a clear tendency among the different field sampling plots that *D* values were significantly affected by the degree of desertification in the investigated area. Generally, wind-induced desertification results in selective removal characterized by clay and silt particle loss; during this coarsening process, *D* values kept decreasing with the increasing degree of soil desertification. Accordingly, in this study, the fixed sand dunes usually had relatively higher *D* values (mean value of 2.4676), whereas lower *D* values were always found in the plots of mobile sand dunes (mean value of 2.1485). Furthermore, semi-mobile sand dunes had medium *D* values (mean value of 2.3243) between the fixed and mobile sand dunes.

Vegetation solutions, not only natural but also artificial, had considerable effects on soil PSD and *D* values as well. Overall, anti-desertification solutions had considerable increases in the fine fractions, and soil PSD recovered more as vegetation ages increased (*e.g.*, Plots 26-28). These functions in soil PSD improvement and *D* value increases are addressed by two activities. On one hand, vegetation restoration solutions consumed erosive forces and carriage ability by increasing aerodynamic roughness lengths and threshold wind velocity, allowing the fine particles to be preserved. Furthermore, biological and physiological activity by vegetation such as photosynthesis, azotification, and litters decomposition also help soil systems to prosper.

In short, fractal dimensions of soil PSD can provide additional information regarding soil degradation among different stages of desertification as well as different solutions for anti-desertification efforts.

3.2 Relationships between fractal dimensions and soil particle contents

Through a log-log transformation, simple linear regression and correlation analyses were performed to identify the strength of correlations between *D* values and the contents of clay, silt, and sand particles (Fig. 1, Table 3). The determination coefficients (R^2) of the linear regressions were high and ranged from 0.50 to 0.81; all the regression analyses passed a two-tailed test indicating the significant difference when evaluated at $p < 0.01$. Specifically, a significant positive correlation occurred between logarithmic *D* values and clay fractions with $R^2 = 0.81$, $P < 0.01$ (Fig. 1A). Figure 1B showed a significant positive correlation between logarithmic *D* values and silt fractions ($R^2 = 0.59$, $P < 0.01$). By contrast, a significant negative correlations was observed, with $R^2 = 0.50$, $P < 0.01$ between logarithmic *D* values and sand
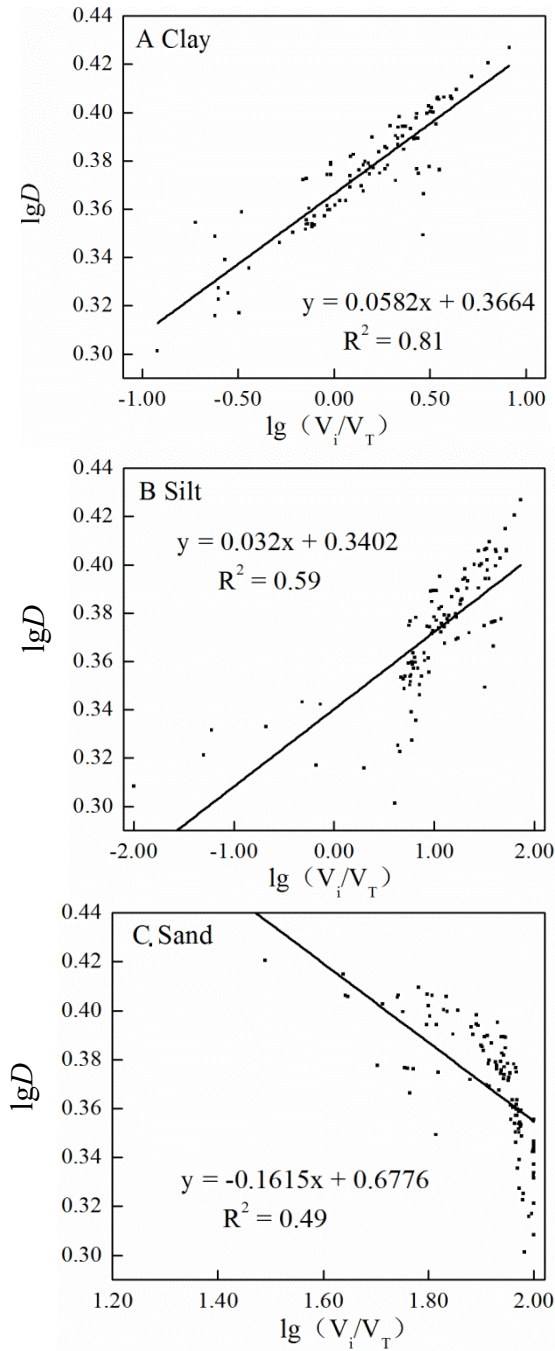
Fig. 1. Relationships between *D* values and soil PSD.

Table 3

Correlation coefficients between *D* values and soil PSD
through a logarithmic transformation

Soil properties	Clay	Silt	Sand
Correlation coefficients	0.900*	0.769*	−0.704*

*)correlation is significant at the 0.01 level (2-tailed)

Table 4

Plots division through a hierarchical cluster analysis

Type	Plots
I	1, 3, 9, 13, 17, 26-28,
II	2, 4-8, 10, 14, 16, 19-20, 29, 33-34, 37
III	11-12, 15, 18, 21-25, 30-32, 35-36, 38-39

fractions (Fig. 1C). This finding indicated that the selected removal of clay and silt fractions resulted in decreasing *D* values. For instance, the highest *D* value was found in Plot 26 which had the highest clay and silt contents (6.58 and 62.41%) and lowest sand content (31.01%); the lowest *D* value corresponded to Plot 22, which had lower clay and silt contents (0.09 and 1.46%) and higher sand content (98.44%). To further identify the relationship between *D* values and desertification, we conducted a hierarchical cluster analysis. The study plots were divided into three types based on *D* values (Table 4). Combining Table 1, the result indicated that Types I and III mainly covered fixed and mobile sand dunes, respectively. Type II was a transitional type, which was composed primarily of semi-mobile dunes. This tendency was also basically consistent with *D* value distribution among area with different degrees of desertification.

Studies regarding soil fractal features are numerous and have led to a much greater understanding of soil environment changes affected by wind erosion in desertified regions. However, although these studies are helpful for estimating variations in soil PSD as well as other soil properties, such as soil organic carbon, nutrients, moisture characteristics, and hydraulic conductivities, fractal models of soil PSD have not been explored in full. Spatial scale effects are one of the most important limitations. In former studies, field investigation always covered an independent and limited area, such as a plateau area, specific mountain, or and even an administrative region (Wang *et al.* 2006, Fu *et al.* 2009, Gao *et al.* 2014a, b). Whereas heterogeneity is a ubiquitous feature of ecological systems; soil properties including soil PSD usually change spatially and temporally (Millán 2007). Therefore, accurate

estimations of soil PSD information with fractal models when scaling up from plots to regions, while maintaining meaningful field-scale process details, remains a challenge. In this study, the sampling plots were all arid, semi-arid, and dry sub-humid regions in northern China. From the east to west, the straight-line distance is more than 3000 km. In this large spatial scale, fractal dimensions still significantly correlated with soil particles, and is demonstrated to be sensitive to soil texture and wind-induced desertification. Breaking the restriction of fractal behavior, it is possible to make reliable assessment of variations in soil PSD indicating soil environment changes at different spatial scales and especially on a large spatial scale.

4. CONCLUSION

In desertified regions of northern China, wind-induced land desertification and vegetation restoration significantly changed the soil PSD. The predominant soil particle sizes concentrated in fine and medium sand fraction classifications accounted for more than 50% of total volume. Fractal analysis showed D values covered a wide range, from 2.0810 to 2.6351. Based on linear regression and correlation analysis, significant positive correlations occurred between logarithmic D values and clay and silt particle contents ($R^2 = 0.81$ and 0.59, $P < 0.01$), in addition to significant negative correlations between logarithmic D values and sand particle content ($R^2 = 0.50$, $P < 0.01$). Hierarchical cluster analysis showed that the sorted plots were similar to sand dune types indicating desertification degree. On a large spatial scale, D was still sensitive to the desertification processes by characterizing soil PSD and its variations. It was suggested that D could be used as a reliable and quantitative parameter to monitor soil systems, and significantly implied land desertification. This improved information contributes to a better understanding of desertification processes in China.

R e f e r e n c e s

Arrouays, D., N. Saby, C. Walter, B. Lemercier, and C. Schvartz (2006), Relation-
    ships between particle-size distribution and organic carbon in French arable
    topsoils, *Soil Use Manage.* **22**, 1, 48-51, DOI: 10.1111/j.1475-2743.2006.
    00020.x.

Buchan, G.D. (1989), Applicability of the simple lognormal model to particle-size
    distribution in soils, *Soil Sci.* **147**, 3, 155-161, DOI: 10.1097/00010694-
    198903000-00001.

Chen, X.H., and Z.H. Duan (2009), Changes in soil physical and chemical properties
    during reversal of desertification in Yanchi County of Ningxia Hui
    autonomous region, *China*, *Environ. Geol.* **57**, 5, 975-985, DOI: 10.1007/
    s00254-008-1382-1.

Chen, Y., and H. Tang (2005), Desertification in north China: Background, anthro-
    pogenic impacts and failures in combating it, *Land Degrad. Develop.* **16**, 4,
    367-376, DOI: 10.1002/ldr.667.

Crawford, J.W., B.D. Sleeman, and I.M. Young (1993), On the relation between
    number-size distributions and the fractal dimension of aggregates, *Eur. J.
    Soil Sci.* **44**, 4, 555-565, DOI: 10.1111/j.1365-2389.1993.tb02321.x.

Ding, G.D. (2010), *Blown Sand Physics*, China Forestry Publishing, Beijng (in Chi-
    nese).

Duan, Z.H., H.L. Xiao, X.R. Li, Z.B. Dong, and G. Wang (2004), Evolution of soil
    properties on stabilized sands in the Tengger Desert, China, *Geomorphol-
    ogy* **59**, 1-4, 237-246, DOI: 10.1016/j.geomorph.2003.07.019.

Fu, H., S.F. Pei, C.G. Wan, and R.E. Sosebee (2009), Fractal dimension of soil par-
    ticle size distribution along an altitudinal gradient in the Alxa rangeland,
    western Inner Mongolia, *Arid Land Res. Manage.* **23**, 2, 137-151, DOI:
    10.1080/15324980902813658.

Gao, G.L., G.D. Ding, B. Wu, Y.Q. Zhang, S.G. Qin, Y.Y. Zhao, Y.F., Bao,
    Y.D. Liu, L. Wan, and J.F. Deng (2014a), Fractal scaling of particle size
    distribution and relationships with topsoil properties affected by biological
    soil crusts, *PLoS One* **9**, 2, e88559, DOI: 10.1371/journal.pone.0088559.

Gao, G.L., G.D. Ding, Y.Y. Zhao, B. Wu, Y.Q. Zhang, S.G. Qin, Y.F. Bao,
    M.H. Yu, and Y.D. Liu (2014b), Fractal approach to estimating changes in
    soil properties following the establishment of Caragana korshinskii shelter-
    belts in Ningxia, NW China, *Ecol. Indic.* **43**, 236-243, DOI: 10.1016/
    j.ecolind.2014.03.001.

Gui, D.W., J.Q. Lei, F.J. Zeng, G.J. Mu, J.T. Zhu, H. Wang, and Q. Zhang (2010),
    Characterizing variations in soil particle size distribution in oasis farmlands
    – A case study of the Cele Oasis, *Math. Comput. Model.* **51**, 11-12, 1306-
    1311, DOI: 10.1016/j.mcm.2009.10.035.

Hillel, D. (1980), *Fundamentals of Soil Physics*, Academic Press, New York,
    413 pp.

Hwang, S.I., K.P. Lee, D.S. Lee, and S.E. Powers (2002), Models for estimating soil particle-size distributions, *Soil Sci. Soc. Am. J.* **66**, 4, 1143-1150, DOI: 10.2136/sssaj2002.1143.

Jiao, F., Z.M. Wen, and S.S. An (2011), Changes in soil properties across a chronosequence of vegetation restoration on the Loess Plateau of China, *Catena* **86**, 2, 110-116, DOI: 10.1016/j.catena.2011.03.001.

Jin, Z., Y.S. Dong, Y.C. Qi, W.G. Liu, and Z.S. An (2013), Characterizing variations in soil particle-size distribution along a grass-desert shrub transition in the Ordos Plateau of Inner Mongolia, China, *Land Degrad. Develop.* **24**, 2, 141-146, DOI: 10.1002/ldr.1112.

Li, X.R., M.Z. He, Z.H. Duan, H.L. Xiao, and X.H. Jia (2007), Recovery of topsoil physicochemical properties in revegetated sites in the sand-burial ecosystems of the Tengger Desert, northern China, *Geomorphology* **88**, 3-4, 254-265, DOI: 10.1016/j.geomorph.2006.11.009.

Liu, X., G.C. Zhang, G.C. Heathman, Y.Q. Wang, and C.H. Huang (2009), Fractal features of soil particle-size distribution as affected by plant communities in the forested region of Mountain Yimeng, China, *Geoderma* **154**, 1-2, 123-130, DOI: 10.1016/j.geoderma.2009.10.005.

Lobe, I., W. Amelung, and C.C. Du Preez (2001), Losses of carbon and nitrogen with prolonged arable cropping from sandy soils of the South African Highveld, *Eur. J. Soil Sci.* **52**, 1, 93-101, DOI: 10.1046/j.1365-2389.2001.t01-1-00362.x.

Mandelbrot, B.B. (1967), How long is the coast of Britain? Statistical self-similarity and fractional dimension, *Science* **156**, 3775, 636-638, DOI: 10.1126/science.156.3775.636.

Mandelbrot, B.B. (1983), *The Fractal Geometry of Nature*, Freeman, New York, 468 pp.

Millán, H. (2007), Scale cutoffs and the limits of fractal soil structure, *Int. Agrophys.* **21**, 2, 169-172.

Nemes, A., J.H.M. Wösten, A. Lilly, and J.H.O. Voshaar (1999), Evaluation of different procedures to interpolate particle-size distributions to achieve compatibility within soil databases, *Geoderma* **90**, 3-4, 187-202, DOI: 10.1016/S0016-7061(99)00014-2.

Reynolds, R.L., M. Reheis, J. Yount, and P. Lamothe (2006), Composition of aeolian dust in natural traps on isolated surfaces of the central Mojave Desert – Insights to mixing, sources, and nutrient inputs, *J. Arid Environ.* **66**, 1, 42-61, DOI: 10.1016/j.jaridenv.2005.06.031.

SFA (2011), A Bulletin of Status Quo of Desertification and Sandification in China, State Forestry Administration of the People's Republic of China, Bejing, http://www.greentimes.com/green/econo/hzgg/ggqs/content/2011-01/05/content_114232.htm (in Chinese).

Skaggs, T.H., L.M. Arya, P.J. Shouse, and B.P. Mohanty (2001), Estimating particle-size distribution from limited soil texture data, *Soil Sci. Soc. Am. J.* **65**, 4, 1038-1044, DOI: 10.2136/sssaj2001.6541038x.

Su, Y.Z., H.L. Zhao, W.Z. Zhao, and T.H. Zhang (2004), Fractal features of soil particle size distribution and the implication for indicating desertification, *Geoderma* **122**, 1, 43-49, DOI: 10.1016/j.geoderma.2003.12.003.

Turcotte, D.L. (1986), Fractals and fragmentation, *J. Geophys. Res.* **91**, B2, 1921-1926, DOI: 10.1029/JB091iB02p01921.

Tyler, S.W., and S.W. Wheatcraft (1990), Fractal processes in soil water retention, *Water Resour. Res.* **26**, 5, 1047-1054, DOI: 10.1029/WR026i005p01047.

Tyler, S.W., and S.W. Wheatcraft (1992), Fractal scaling of soil particle-size distribution: analysis and limitations, *Soil Sci. Soc. Am. J.* **56**, 2, 362-369, DOI: 10.2136/sssaj1992.03615995005600020005x.

UNEP (1994), United Nations Convention to combat desertification in those countries experiencing serious drought and/or desertification, particularly in Africa, United Nations Environment Programme for the Convention to Combat Desertification (CCD), Interim Secretariat for the CCD, Switzerland, Geneva, 71 pp.

Wang, G.L., S.L. Zhou, and Q.G. Zhao (2005), Volume fractal dimension of soil particles and its applications to land use, *Acta Pedol. Sin.* **42**, 4, 545-550.

Wang, X.D., M.H. Li, S.Z. Liu, and G.C. Liu (2006), Fractal characteristics of soils under different land-use patterns in the arid and semiarid regions of the Tibetan Plateau, China, *Geoderma* **134**, 1-2, 56-61, DOI: 10.1016/j.geoderma. 2005.08.014.

Wang, X.M., F.H. Chen, E. Hasi, and J.C. Li (2008), Desertification in China: An assessment, *Earth-Sci. Rev.* **88**, 3-4, 188-206, DOI: 10.1016/j.earscirev. 2008.02.001.

Zha, Y., and J. Gao (1997), Characteristics of desertification and its rehabilitation in China, *J. Arid Environ.* **37**, 3, 419-432, DOI: 10.1006/jare.1997.0290.